

Analyzing the Intracavity Frequency Doubling of the Simultaneous Q -Switched Mode-Locked Diode-Pumped Pulsed Nd^{3+} Laser with $\text{Cr}^{4+}:\text{YAG}$ as a Polarized Saturable Absorber

B. ABDUL GHANI* AND M. HAMMADI

Atomic Energy Commission, P.O. Box 6091, Damascus, Syria

(Received October 26, 2010; in final form January 19, 2011)

The intracavity frequency doubling of a simultaneous passively Q -switched mode-locked diode-pumped Nd^{3+} laser is studied with a polarized isotropic $\text{Cr}^{4+}:\text{YAG}$ saturable absorber. A general recurrence formula for the mode-locked pulses under the Q -switched envelope at a fundamental wavelength has been reconstructed in order to analyze the temporal shape behaviour of a single Q -switched envelope with mode-locking pulse trains. This formula has been derived taking into account the impact of the intracavity frequency doubling and polarized $\text{Cr}^{4+}:\text{YAG}$ saturable absorber (the Fresnel losses). The presented mathematical model essentially describes the self-induced anisotropy appearing in the polarized $\text{Cr}^{4+}:\text{YAG}$ in the nonlinear stage of the giant pulse formation. For the anisotropic $\text{Nd}^{3+}:\text{YVO}_4$ active medium, the generated polarized waves are fixed through the lasing cycle. Second harmonic peak power, pulse width, pulse duration, shift pulse position of central mode and rotational angle as a function of the absorber initial transmission are estimated. The calculated numerical results are in good qualitative and quantitative agreement with the available experimental data reported in references.

PACS: 42.55.Px, 42.55.Rz, 42.68.Mj

1. Introduction

Q -switching and simultaneous mode-locking processes should be of a great interest for the generation of the ultrashort output laser pulses with high peak power. The high output peak power is beneficial to wavelength conversion in an external and internal nonlinear KTP crystal [1, 2]. The emitted output Nd^{3+} laser pulse trains can be used to study the dynamic optical nonlinearities in the range of 100–1000 nm. Intracavity frequency doubling (IFD) Nd^{3+} laser sources with high peak power, moderated averaged power and high repetition rate are useful in surgery, angioplasty and dermatology as well as in different branches of science and technology such as coherent telecommunication and information storage [2–4].

Achieving passive Q -switching and mode-locking Nd^{3+} laser pulses by organic dye cells exhibit poor stability, due to low heat conductivity, photodissociation and burning in the laser field. Passive Q -switched polarized and mode-locked $\text{Cr}^{4+}:\text{YAG}$ crystal shows a great interest, in comparison with the use of active methods involving costly acousto-optic modulator, because it involves less complexity and low cost, reliability and simplicity in fabrication [5].

The $\text{Cr}^{4+}:\text{YAG}$ based saturable absorbers seem to be preferred in comparison with other absorbers such as $\text{LiF}:\text{F}_2^-$, due to their properties related to active ions,

mainly improved thermomechanical properties, large absorption cross-section near 1064 nm, relatively high concentration, moderate excited state lifetime and low saturable fluence at 1064 nm [5, 6].

The saturation of the excited state absorption in polarized isotropic $\text{Cr}^{4+}:\text{YAG}$ crystal is responsible for the mode-locking process, since this state has a very short lifetime. The $\text{Nd}^{3+}:\text{YVO}_4$ laser is favorable candidate for mode-locking process, due to its larger gain band width in comparison with $\text{Nd}^{3+}:\text{YAG}$ laser.

When the saturation absorption in $\text{Cr}^{4+}:\text{YAG}$ becomes significant, the polarization characteristics can be formed at the stage of growth of a giant laser pulse. The self-induced polarization anisotropy in the cavity appears due to the self-induced anisotropy of the saturation absorption and the self-induced changes in polarization within the cavity. Changing the angular position of $\text{Cr}^{4+}:\text{YAG}$ switch in the cavity altered the degree of ellipticity of the polarization. The appearance of the polarization ellipticity ϵ is related to the self-induced birefringence in the $\text{Cr}^{4+}:\text{YAG}$ crystal during the stage of the absorption saturation [7].

The problem of passively Q -switched lasers with simultaneous mode-locking has been treated experimentally and theoretically in many references [1–6, 8–10] with, and without the existence of the IFD. None of the mentioned references discusses the impact of the polarization process on the characteristics of the output laser pulse.

A simple and reliable mathematical treatment of the passively Q -switched Nd^{3+} laser with simultaneous mode-locking is demonstrated in this work. The influ-

* corresponding author; e-mail: pscientific@aec.org.sy

ence of the IFD (green laser) and the polarization (the Fresnel losses) of a Cr^{4+} :YAG saturable absorber have been taken into consideration in the developed mathematical model. The concepts of peak symmetry factor and build-up time are used to describe the laser pulse shape quantitatively.

This work also concentrates on the influence of the polarized Cr^{4+} :YAG crystal angular position on the Q-switched simultaneously mode-locked laser density.

2. Analyzing the problem

The coupled rate equation for the fundamental photon density in IFD passively Q-switched and simultaneously mode-locked lasers by considering the influence of intracavity focusing, the excited state absorption effect and polarization of the Cr^{4+} :YAG isotropic crystal (the Fresnel losses, Figs. 1 and 2) can be written as follows [2, 3, 5, 6, 9, 11, 12]:

$$\begin{aligned} \frac{dU_Q}{dt} = \frac{U_Q}{t_r} \left\{ \left[2\sigma N\ell - 2\sigma_{\text{GS}}N_1^s\ell_s \cos^2(\vartheta - \varphi) \right. \right. \\ \left. \left. - 2\sigma_{\text{ES}}N_2^s\ell_s \sin^2(\vartheta - \varphi) \right] - \eta_{2\omega}vW_pU_Q \right. \\ \left. - \left[\ln\left(\frac{1}{R}\right) + \rho_{\text{ns}} + \alpha_x \cos^2\varphi + \alpha_y \sin^2\varphi \right] \right\}, \quad (1) \end{aligned}$$

where $t_r = 2L_{\text{eff}}/c$ is the photon round trip time in the cavity, c is the light velocity in vacuum, $L_{\text{eff}} = [n_g\ell + n_s\ell_s + n_1^{\omega}\ell_c + (L - \ell - \ell_s - \ell_c)]$ is the effective optical length of resonator, n_g is the refractive index of gain medium, ℓ is the length of the gain medium, n_s is the refractive index of polarized Cr^{4+} :YAG saturable absorber, ℓ_s is the thickness of the saturable absorber, n_1^{ω} is the refractive index of the nonlinear KTP element, ℓ_c is the thickness of the KTP crystal, L is the resonator length, σ is the stimulated emission cross-section of the gain medium, N is the population density of the gain medium, σ_{GS} and σ_{ES} are the ground and excited state absorption cross sections of the polarized saturable absorber, respectively, N_1^s and N_2^s are the population densities of the ground and first excited state of polarized isotropic Cr^{4+} :YAG crystal, respectively, ϑ and φ are the rotational and polarization angles, respectively, R is the reflection coefficient of the output cavity mirror, ρ_{ns} are the non-saturable intracavity round trip dissipative losses, α_x and α_y are the Fresnel losses on the x and y axis, respectively, $\eta_{2\omega}$ is the impact of the IFD, $v = c/n_1^{\omega}$ is the light velocity in KTP crystal and W_p is the energy of the fundamental photon.

By assuming that the excited state lifetime of the absorber is larger than the laser pulse width, the instantaneous population inversion density of the uniform-pumped gain medium, in each period of pulse build-up, can be written in the following reduced form [2, 3, 5, 6, 9]:

$$\frac{dN}{dt} = -\gamma\sigma cU_QN, \quad (2)$$

where γ is the inversion reduction factor ($\gamma = 1$ and

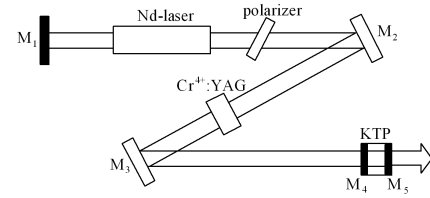


Fig. 1. Experimental setup of the IFD simultaneously Q-switched and mode-locked diode-pumped Nd^{3+} laser with polarized Cr^{4+} :YAG saturable absorber [3].

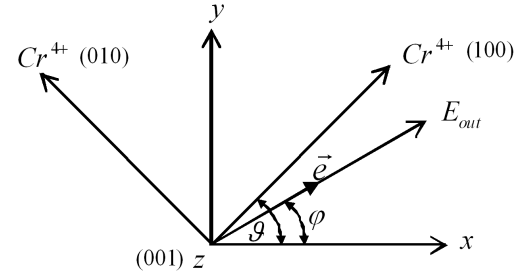


Fig. 2. Angular orientations of Cr^{4+} :YAG crystal axes ($\vartheta, \vartheta + \pi/2$) and polarization angle of the electrical field $E_{\text{out}}(\varphi)$ (with resonantly absorbing dipoles) of the output laser pulse.

$\gamma = 2$ correspond to four and three-level laser system, respectively).

A desirable condition for a good-pulsed mode-locking is that the saturable absorber should have enough short lifetime to recover its absorption process between individual noise bursts. Under this condition, the preferred pulse does not bring up several closely following noise spikes along with it.

The relaxation time of it is in the microsecond region, which generally would not be allowed to obtain mode-locking. Nevertheless, when the intracavity intensity is high enough, all of the Cr^{4+} ions are quickly excited to the first excited state, and strong excited state absorption causes a great quantity of Cr^{4+} ions to accumulate in higher-lying levels. Since the relaxation time of the excited state absorption is relatively short ($\tau_{\text{es}} = 0.1$ ns) [5], passive mode-locking with a Cr^{4+} :YAG saturable absorber would be possible if strong intensity fluctuations are introduced. Another important condition is that the build-up time of the Q-switched pulse must be sufficiently short due to the limitation of the round trip time of the density fluctuation [5].

The time evolution of instantaneous population inversion density of the ground level of polarized isotropic Cr^{4+} :YAG saturable absorber, neglecting the different relaxation process, is [2, 3, 5, 6, 9]:

$$\frac{dN_1^s}{dt} = -\frac{Ac}{A_s}\sigma_{\text{GS}}U_QN_1^s \cos^2(\vartheta - \varphi), \quad (3)$$

where A and A_s are the average laser beam cross-sections at the gain and the absorber media, respectively.

Presence of $\cos^2(\vartheta - \varphi)$ and $\sin^2(\vartheta - \varphi)$ functions in Eqs. (1) and (3) makes the mathematical model essentially sensitive to the self-induced anisotropy appearing in the nonlinear stage of the giant output pulse formation [7, 13]. This holds for any position of Cr⁴⁺:YAG absorber relatively to the orientation of a Nd:YVO₄ crystal, which dictates the linear state of polarization established in lasers. For the anisotropic Nd:YVO₄ active medium, the generated polarized waves with resonantly absorbing dipoles are fixed through the lasing cycle. So, the nonlinear polarization rotational effect, observed in lasers based on the Nd³⁺ active medium garnet, is fully eliminated [13].

In order to make the above mentioned analysis simpler, suppose that the cuts of YAG crystalline host is positioned in the cavity along (001), so that the light propagates along (001) crystallographic axis, while the laser polarization azimuth is kept fixed (given by the orientation of the Nd:YVO₄) and, of course, orthogonal to this direction [13] (Fig. 2).

The orientations of the x and y axes are chosen so that the total cavity losses are in their minimum along x axis and in their maximum along y axis. It means that the axis [001] (Fig. 2) can be chosen to be parallel to the optical axis of the laser beam. The other two axes [100] and [010] are oriented with respect to the optical axis z at the angle ϑ and $\vartheta + \pi/2$, respectively [7].

The polarization state of a Nd³⁺ laser passively Q-switched with polarized Cr⁴⁺:YAG is generally governed by the relative orientations of the Cr⁴⁺:YAG crystal and the intracavity partial polarizer as well as by the density of a giant laser pulse in the switch [7].

For the plane parallel resonator with circular aperture and for a relatively large Fresnel number $N_F \geq 1$, the Fresnel losses of the tilted glass plate (polarizer) are given by the following relation [7, 14]:

$$\alpha_y = 8\delta(M + \delta)K_{pk}^2 / [(M + \delta)^2 + \delta^2], \quad \delta = 0.824,$$

$$M = (8\pi N_F)^{1/2}, \quad (4)$$

where $K_{pk}^2 = (j\frac{\pi}{2})^2 \exp(j(p + \ell)\frac{\pi}{2})H_p^{(1)}(x)H_k^{(1)}(x)$ is the $(p + k)$ -th zero of the Macdonald (Bessel) function of order k , $j = \sqrt{-1}$ and $H_p^{(1)}(x)$ is the Hankel function of order p [15].

The phenomena of mode-locking in a passive Q-switched laser pulse achieved by polarized solid state Cr⁴⁺:YAG saturable absorber can be explained by the fluctuation mechanism. There are two stages of the pulse formation, due to the mentioned mechanism. The linear stage of the fluctuation laser intensity is generated due to the interference of the large number of modes into the cavity. The nonlinear stage is referred to the bleaching process in the polarized Cr⁴⁺:YAG saturable absorber. Most of the compressed intensive fluctuation of laser peaks can be amplified faster than the weaker ones in the nonlinear stage [2, 3]. The peaks of the laser pulses cannot be much compressed during the time after subsequent round trips. The shape of the total photon

density can then be written as

$$U_Q(t) = \sum_{k=0} U_k f(t - t_k), \quad (5)$$

with

$$\int_{-\infty}^{+\infty} c\sigma f(t) dt = 1, \quad (6)$$

where $t_k = kt_r$, t_r is the round trip time in the cavity, U_k is the relative amplitude of the mode-locked output laser pulse at the k -th round trip and the function $f(t)$ is the normalized sharp pulse function centered at $t = 0$ of mode-locked pulse generated from the noise, which must fall rapidly in a time shorter than the resonator transit time.

The shape of the laser pulse passively mode-locked by polarized Cr⁴⁺:YAG saturable absorber can be described by a hyperbolic secant square function. Assuming that the function $f(t)$ is from the following shape [2, 3]:

$$f(t) \propto \text{sech}^2(t/\tau_p) = \frac{1}{2c\sigma\tau_p} \text{sech}^2(t/\tau_p), \quad (7)$$

where $\tau_p = \frac{1}{1.76}$ (FWHM) and FWHM is the mode-locked pulse width.

The relative amplitude of the mode-locked laser pulses at time t_k , after an additional round trip, using Eq. (1) is given as follows [2]:

$$\begin{aligned} U_k = U_{k-1} \exp & \left(2\sigma N(t_k)\ell - 2 \left[\sigma_{GS} N_1^s(t_k)\ell_s \right. \right. \\ & \times \cos^2(\vartheta - \varphi) + \sigma_{ES} N_2^s(t_k)\ell_s \sin^2(\vartheta - \varphi) \\ & \left. \left. - \left[\ln \left(\frac{1}{R} \right) + \rho_{ns} + \alpha_x \cos^2 \varphi + \alpha_y \sin^2 \varphi \right] \right) \right) \\ & - U_{k-1} \exp(-\rho_{KTP} U_{k-1}), \end{aligned} \quad (8)$$

where $\rho_{KTP} = \frac{\eta_{2\omega}}{6} \frac{A}{A_c} \frac{W_p}{\sigma\tau_p}$ is the loss in the KTP crystal [3].

The formula (8) can be rewritten as

$$\begin{aligned} U_k = U_{k-1} \exp & \left(2\sigma N(t_k)\ell - \left[2(1 + \beta)\sigma_{GS} N_1^s \ell_s \right. \right. \\ & \times \cos^2(\vartheta - \varphi) - 2\beta\sigma_{GS} N_1^s \ell_s + \beta \ln \left(\frac{1}{T_0^2} \right) \\ & \left. \left. - \left[\ln \left(\frac{1}{R} \right) + \rho_{ns} + \alpha_x \cos^2 \varphi + \alpha_y \sin^2 \varphi \right] \right) \right) \\ & - U_{k-1} \exp(-\rho_{KTP} U_{k-1}), \end{aligned} \quad (9)$$

where $N_1^s(t_k) + N_2^s(t_k) = N_0^s$, $\beta = \sigma_{ES}/\sigma_{GS}$ and $T_0 = \exp(-\sigma_{GS} N_0^s \ell_s \sin^2(\vartheta - \varphi))$ is the polarized absorber's initial transmission.

Using the form of T_0 , the polarization angle of the giant laser pulse can be determined by the following relation:

$$\varphi = \vartheta - \arcsin \sqrt{\ln(1/T_0)/\sigma_{GS}N_0^s\ell_s}. \quad (10)$$

Dividing Eq. (2) by N , using relations (5) and (6) and integrating over time from zero to t_k , $N(t_k)$ will be given as follows [2, 3, 16, 17]:

$$N(t_k) = N_i \prod_{m=0}^{k-1} \exp(-\gamma U_m), \quad (11)$$

where N_i is the initial population inversion density at the starting point of the Q-switching process. By setting $N = N_i$, $N_1^s = N_0^s$, $\frac{dU_Q}{dt} = 0$ in Eq. (1), the initial population inversion density can be given by the following relation:

$$N_i = \frac{1}{2\sigma\ell} \left[\ln(1/T_0^2) + \ln(1/R) + \rho_{ns} + \alpha_x \cos^2 \varphi + \alpha_y \sin^2 \varphi \right]. \quad (12)$$

Dividing the rate Eq. (2) by Eq. (3) and integrating gives [2, 3, 16, 17]:

$$N_1^s(t_k) = N_0^s \left[\frac{N(t_k)}{N_i} \right]^\xi, \quad (13)$$

where the parameter $\xi = \frac{\sigma_{GS}}{\sigma\gamma} \frac{A}{A_s} \cos^2(\vartheta - \varphi)$ indicates how fast is the saturable absorber bleaching.

By substituting (11), (12) and (13) into (9), the reconstructed recurrence formula for the relative amplitude of the mode-locked output laser pulse at the k -th round trip will be given as follows [3]:

$$U_k = U_{k-1} \exp \left(\left[\prod_{m=0}^{k-1} \exp(-\gamma U_m) - 1 \right] \times \left[\ln \left(\frac{1}{R} \right) + \rho_{ns} + \alpha_x \cos^2 \varphi + \alpha_y \sin^2 \varphi \right] + \left[\prod_{m=0}^{k-1} \exp(-\gamma U_m) - \left[\beta + (1 - \beta) \left(\prod_{m=0}^{k-1} \exp(-\gamma U_m) \right)^\xi \right] \right] \times \ln \left(\frac{1}{T_0^2} \right) - \rho_{KTP} U_{k-1} \right). \quad (14)$$

Considering the bidirectional propagation of the fundamental beam in the laser cavity, the power of mode-locked fundamental pulse can be written by the following relation [2, 3, 6]:

$$P_\omega = \frac{A}{2} \left(\frac{W_p}{2\sigma\tau_p} \right) \ln \left(\frac{1}{R} \right) \sum_{k=0}^{\infty} U_k \operatorname{sech}^2 \left(\frac{t-t_k}{\tau_p} \right). \quad (15)$$

Then the second harmonic (SH) power under the small-signal approximation is given by [2, 3]:

$$P_{2\omega} = \eta_{2\omega} \frac{P_\omega^2}{A}$$

$$= \frac{3}{2} A \left(\frac{W_p}{2\sigma\tau_p} \right) \rho_{KTP} \sum_{k=0}^{\infty} U_k^2 \operatorname{sech}^4 \left(\frac{t-t_k}{\tau_p} \right). \quad (16)$$

Finally, the total output green pulse energy (532 ns) of the Q-switched mode-locked is given by the following relation [2, 3, 6]:

$$E_{2\omega} = \frac{W_p}{\sigma} \frac{A^2}{A_c} \rho_{KTP} \sum_{k=0}^{\infty} U_k^2. \quad (17)$$

3. Results and discussion

It should be mentioned here that the calculated results, in this work, are generated using the recurrence formula (14) and the parameters values reported in Table I.

TABLE I

Physical constants and geometrical parameters of the IFD of simultaneous Q-switched and mode-locked Nd³⁺:YVO₄ laser with polarized Cr⁴⁺:YAG saturable absorber.

Constant	Value	Unit	Constant	Value	Unit
σ	25×10^{-19}	cm ²	n_s	1.82	–
σ_{GS}	70×10^{-19}	cm ²	n_1^ω	1.83	–
β	0.28	–	n_g	1.82	–
A	0.322×10^{-2}	cm ²	ℓ	0.15	cm
A/A_s	20–30	–	ℓ_s	0.3	cm
A/A_c	1.14	–	ℓ_c	0.5	cm
ρ_{ns}	0.01	–	L	42	cm
R	0.998	–	d_{eff}	3.66	pm/V
τ_p	400	ps	T_0	0.81	–
γ	1	–	U_0	10^{-3}	–
$\eta_{2\omega}$	1.54×10^{-8}	cm ² /W	α_x	0.04	–
W_p	1.86×10^{-19}	J	α_y	0.24	–

Figure 3 shows the relative amplitude U_k of the IFD Q-switched simultaneously mode-locked output laser pulse as a function of m -th round trip. Closely good symmetry of the amplified noise in the laser cavity can be noticed.

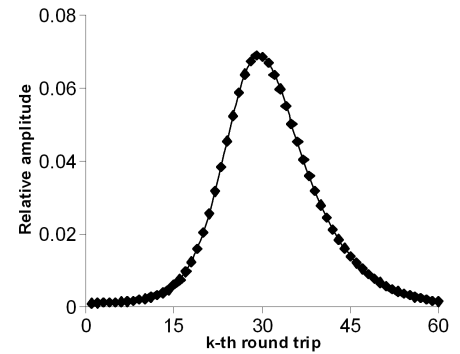


Fig. 3. Relative amplitude U_k of the IFD Q-switched simultaneously mode-locked output laser pulse as a function of m -th round trip.

The temporal behavior of the SH pulse power for different values of the absorber initial transmission is demonstrated in Fig. 4. These results are obtained for 99.8%

of output mirror reflectivity and rotational angle of 65° . It can be seen from Fig. 4 and Table II that by increasing the absorber initial transmission, the build-up time and the number of amplified noise are increased, while the maximum SH power and pulse symmetry factor are decreased. The decrement of the pulse symmetry factor (Table II) is due to the increment of the KTP nonlinear conversion, and it is beneficial to avoid the undesired birefringent effects. The separation time of the mode-locked pulses within the Q -switched envelope is about 2.8×10^{-9} s (Fig. 4), which exactly matches the transit time of the cavity round trip ($t_r = 2L/c$).

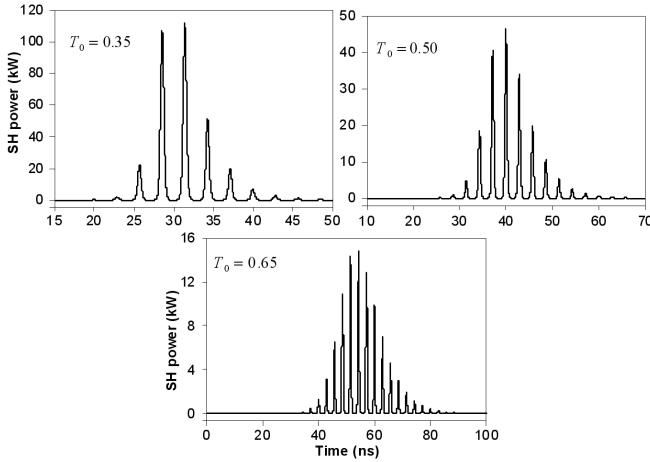


Fig. 4. Temporal behavior of a single Q -switched and simultaneous mode-locked SH pulse power for different values of absorber initial transmission, and 99.8% of output mirror reflectivity and rotational angle of 65° .

TABLE II

Build-up time, pulse symmetry factor and SH power of a single Q -switched and simultaneous mode-locked laser pulse for different values of the absorber initial transmission.

T_0	Build-up time [ns]	Pulse symmetry factor	SH pulse power [kW]
0.35	31	1.6	119.5
0.50	39	1.2	47.5
0.65	53	1.1	15.1

Figure 5 shows the SH peak power of central mode as a function of rotational angle of the polarized $\text{Cr}^{4+}:\text{YAG}$ isotropic crystal for different values of the absorber initial transmission. It can be seen from this figure that at high laser transmission, the maximum SH peak powers tends closely to isotropic state. The decrement of the absorber initial transmission leads to the increment in the SH peak power. Therefore, the optical Cr^{4+} active centers become steadily saturated and the anisotropic behavior clearly appears.

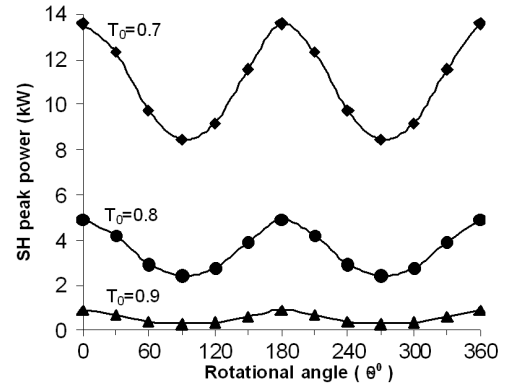


Fig. 5. Central mode SH peak power versus polarized crystal rotational angle for different values of initial transmission.

As the laser radiation propagates along $[001]$ optical axis (Fig. 2), the power required for saturation must be at its maximum. This happens when the transition is at its minimum and the SH power at its maximum. This means that the electric vector is parallel to either $[010]$ or $[100]$ transition moments for $\vartheta = 0^\circ, 180^\circ$, and 360° , respectively. In this case, only one subset (one-third) of the total active centers participates in the laser action; and for $\vartheta = 90^\circ, 270^\circ$ two subsets (two-third) of the total active centers with $[010]$ and $[100]$ moments are simultaneously participating in the laser action. This qualitatively interprets the peaks behavior and troughs appearing in Fig. 5.

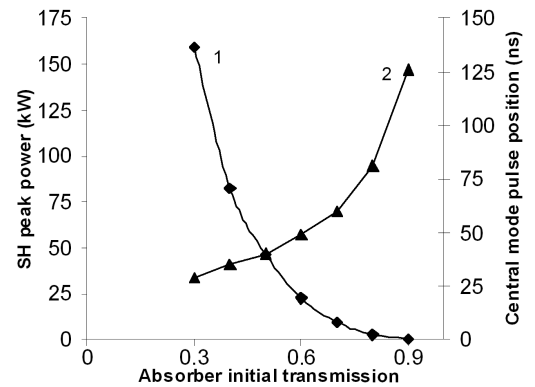


Fig. 6. Power peaks (1) and central mode pulse position (2) as a function of initial transmission.

Figure 6 shows the SH power peaks (line 1) and the central mode pulse position (line 2) as a function of the absorber initial transmission for rotational angle of 65° . The decrement of the SH peak power caused by the increment of the absorber initial transmission may be due to the limitation of the KTP conversion efficiency at high laser pulse density.

In order to see the effect of mode-locked pulse width on the SH peak power at the central of the Q -switched envelope

lope, the peak power at constant rotation angle is plotted as a function of τ_p (Fig. 7). It can be seen from this figure that the SH peak power depends inversely on τ_p .

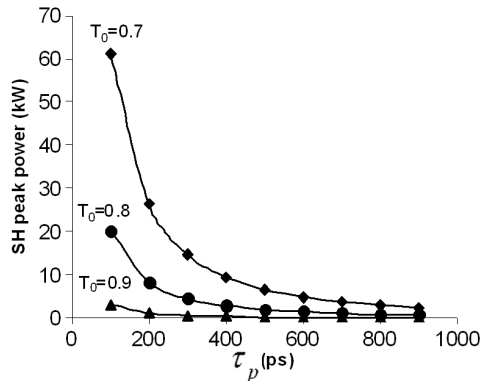


Fig. 7. SH peaks power of the central mode as a function of τ_p for different values of the absorber initial transmission.

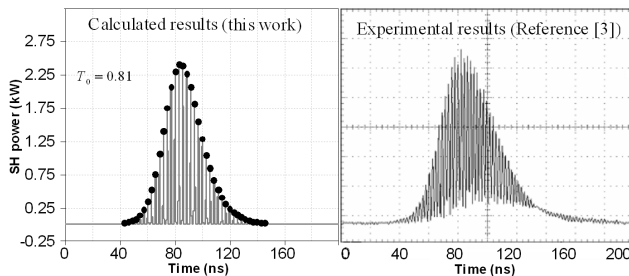


Fig. 8. Calculated (this work) (a) and experimental results [3] (b) for the time dependence of the Q-switched second harmonic pulse power.

Finally, a comparison between the calculated, in this work, and experimental SH power reported in Ref. [3] is demonstrated in Fig. 8. The SH power of mode-locked pulse at the central peak of the Q-switched envelope is calculated for absorber initial transmission of 0.81 and rotational angle of 65° . The reported measured and calculated values of the SH peak power are 2.4 kW, 2.7 kW, respectively [3], while the calculated power, in this work, reaches 2.4 kW. Besides, the peak values of the mode-locked pulses after normalization them to their highest values correspond with the calculated profiles. It can also be seen from Fig. 8 that the rising part of the calculated Q-switched envelope has excellent matching with the measured profile of the relative amplitude reported in [3]. The slight mismatch in the falling part may be due to the imprecise estimation of the intracavity losses. The calculated pulse width of the Q-switched envelope reaches 46 ns in this work, whereas the experimental value reported in Ref. [3] is 47 ns.

4. Conclusion

This work demonstrates the use of an isotropic polarized Cr^{4+} :YAG crystal in the IFD of a simultaneous Q-switched and mode-locked diode-pumped Nd:YVO₄ laser. Nonlinear and the Fresnel losses have been taken into consideration in the laser system. For the anisotropic Nd:YVO₄ active medium, the generated polarized waves are fixed through the lasing cycle of Cr^{4+} :YAG saturable absorber.

The calculated numerical results show good quantitative and qualitative consistency with the available experimental data. The presented mathematical model, in this work, can be used to investigate other Nd³⁺ lasers such as Nd:YAG, Nd:GdVO₄, etc.

Acknowledgments

The authors would like to express their thanks to the Director General of AECS Prof. I. Othman for his continuous encouragement, guidance and support.

References

- [1] P.K. Mukhopadhyay, M.B. Alsous, K. Ranganathan, S.K. Sharma, P.K. Gupta, A. Kuruvilla, T.P.S. Nathan, *Opt. Laser Technol.* **37**, 157 (2005).
- [2] Y.F. Chen, J.L. Lee, H.D. Hsieh, S.W. Tsai, *IEEE J. Quant. Electron.* **38**, 312 (2002).
- [3] P.K. Mukhopadhyay, M.B. Alsous, K. Ranganathan, S.K. Sharma, P.K. Gupta, J. George, T.P.S. Nathan, *Appl. Phys. B: Lasers Opt.* **79**, 713 (2004).
- [4] P.K. Mukhopadhyay, M.B. Alsous, K. Ranganathan, S.K. Sharma, P.K. Gupta, J. George, T.P.S. Nathan, *Opt. Commun.* **222**, 399 (2003).
- [5] Y.F. Chen, S.W. Tsai, *IEEE J. Quant. Electron.* **37**, 580 (2001).
- [6] J. Liu, D. Kim, *IEEE J. Quantum Electron.* **35**, 1724 (1999).
- [7] B. Abdul Ghani, M. Hammadi, *Acta Phys. Pol. A* **115**, 873 (2009).
- [8] J.Y. Peng, H.M. Tan, Y.G. Wang, B.S. Wang, J.G. Miao, L.S. Qian, X.Y. Ma, *Solid State Liquid Lasers* **16**, 1601 (2006).
- [9] Y.F. Chen, Y.P. Lan, H.L. Chang, *IEEE J. Quantum Electron.* **37**, 460 (2001).
- [10] X. Zhang, S. Zhao, Q. Wang, B. Ozygus, H. Weber, *IEEE J. Quantum Electron.* **35**, 1912 (1999).
- [11] J. Liu, D. Shen, S.C. Tam, Y.L. Lam, *IEEE J. Quantum Electron.* **37**, 888 (2001).
- [12] G. Li, S. Zhao, K. Yang, J. Liu, *Opt. Mater.* **27**, 719 (2005).
- [13] E.R. Villiafana, A.V. Kir'yanov, *Opt. Commun.* **242**, 241 (2004).
- [14] W. Koehner, *Solid-State Laser Engineering*, 6th ed., Springer Verlag, Berlin 2005.
- [15] B.G. Korenev, *Introduction to Theory of the Bessel Function*, Nakladatelvi Technicke Literatry, Prague 1977 (Czech language).
- [16] J.J. Degnan, *IEEE J. Quantum Electron.* **31**, 1890 (1995).
- [17] Y.S. Huang, F.L. Chang, *Opt. Rev.* **12**, 396 (2005).